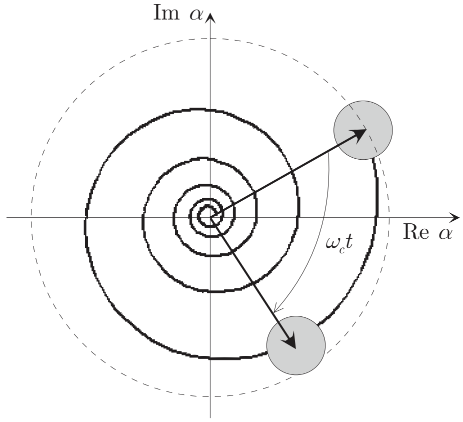

Fig. 3.14 Pictorial representation of the time evolution of a relaxing coherent state.

Note that the environment modes also contain at any time coherent states resulting from the accumulation of tiny coherent amplitudes along the successive time intervals. The global mode–environment state can be written as:

$$|\alpha e^{-\kappa t/2}\rangle \prod_i |\beta_i\rangle \ , \tag{3.138}$$

where the partial amplitudes β_i are such that:

$$\sum_i |\beta_i|^2 = \overline{n}(1 - e^{-t/T_c}) \ , \tag{3.139}$$

a relation resulting simply from the total energy conservation.

The derivation presented here is heuristic and qualitative. Its conclusions are correct though, as a much more rigorous description of coherent state damping will prove in Section 4.4.4. We will come back to the analysis of field relaxation in terms of linear coupling with a large set of oscillators in Chapter 7, when dealing with the decoherence of mesoscopic superpositions of coherent states.[22]

3.3 The spin system

We have, in the previous sections, described springs, either isolated or in mutual interaction. Although this physics is rich, these models are not sufficient to describe the variety of effects encountered in quantum optics. We must introduce another player in the game, the spin system. This section briefly recalls useful notation, only partly introduced in Chapter 2, and describes how classical fields provide tools to manipulate individual spin states using techniques borrowing amply from nuclear magnetic resonance.

3.3.1 A two-level atom

We consider a two-level atom whose upper level $|e\rangle$ is connected to level $|g\rangle$ by an electric dipole transition at angular frequency ω_{eg}. This system is equivalent to a spin-$1/2$ evolving in an abstract space, with a magnetic field oriented along the 'vertical' Z

[22]See also the appendix, which describes field damping using the formalism of the field characteristic function.

axis accounting for the energy difference between $|e\rangle$ and $|g\rangle$. These states correspond to the eigenstates of the spin along Z, which we denote, as in Chapter 2, by $|0\rangle$ and $|1\rangle$. The assignment of $|e\rangle$ and $|g\rangle$ with qubit states is of course arbitrary. Here we will make the correspondence $|e\rangle \to |0\rangle$ and $|g\rangle \to |1\rangle$, which, with the conventions of quantum information, make $|e\rangle$ and $|g\rangle$ eigenstates of σ_Z with eigenvalue $+1$ and -1 respectively, the atomic Hamiltonian being:

$$H_a = \frac{\hbar\omega_{eg}}{2}\sigma_Z \ , \tag{3.140}$$

where we have set the zero of energy half-way between the two levels. Note that the chosen qubit assignment means that the state $|1\rangle$ is less excited than the state $|0\rangle$, which can be surprising. In some cases, it might be more convenient to use the opposite qubit choice and we will in the following shift freely from one qubit definition to the other.

Let us introduce also the atomic raising and lowering operators $\sigma_\pm$:

$$\sigma_\pm = \tfrac{1}{2}(\sigma_X \pm i\sigma_Y) \ . \tag{3.141}$$

In terms of the spin eigenstates along the Z axis, these operators are:

$$\sigma_+ = |0\rangle\langle 1| \ ; \qquad \sigma_- = \sigma_+^\dagger = |1\rangle\langle 0| \ . \tag{3.142}$$

It follows that:

$$\sigma_+|1\rangle = |0\rangle \ ; \qquad \sigma_-|0\rangle = |1\rangle \ ; \qquad \sigma_+|0\rangle = 0 \ ; \qquad \sigma_-|1\rangle = 0 \ . \tag{3.143}$$

These atomic excitation creation/annihilation operators have a fermionic commutation relation:

$$[\sigma_-, \sigma_+]_+ = 1 \ , \tag{3.144}$$

where $[,]_+$ denotes an anti-commutator. This relation results from the fact that the atom carries at most one excitation. There is a clear analogy between $\sigma_\pm$ and the photon creation and annihilation operators defined in Section 3.1.1. The atomic Hamiltonian is in terms of these operators:

$$H_a = \hbar\omega_{eg}(\sigma_+\sigma_- - \sigma_-\sigma_+)/2 = \hbar\omega_{eg}(\sigma_+\sigma_- - \mathbb{1}/2) \ . \tag{3.145}$$

3.3.2 Manipulating a spin-½ with a classical field

Being able to prepare or analyse the spin in a state corresponding to an arbitrary point on the Bloch sphere is essential in the quantum optics experiments described below. This is achieved by realizing rotations on the Bloch sphere induced by classical fields, resonant or quasi-resonant with the atomic transition. According to eqns. (3.33) and (3.34), these unitary operations result from the action of the atom–field Hamiltonian:

$$H = H_a + H_r \ , \tag{3.146}$$

where:

$$H_r = -\mathbf{D}\cdot\mathbf{E}_r \ , \tag{3.147}$$

describes the coupling of the atomic dipole operator, $\mathbf{D} = q\mathbf{R}$, with the classical time-dependent electric field:

$$\mathbf{E}_r = i\mathcal{E}_r \left[\boldsymbol{\epsilon}_r e^{-i\omega_r t} e^{-i\varphi_0} e^{-i\varphi} - \boldsymbol{\epsilon}_r^* e^{+i\omega_r t} e^{i\varphi_0} e^{i\varphi}\right] \; . \tag{3.148}$$

In this equation, $\mathcal{E}_r$ is the real amplitude of the classical field, ω_r its angular frequency, $\boldsymbol{\epsilon}_r$ the complex unit vector describing its polarization and $\varphi+\varphi_0$ its phase (its splitting in two parts is explained below).

Assuming that $|0\rangle$ and $|1\rangle$ are levels of opposite parities, the odd-parity $q\mathbf{R}$ dipole operator is purely non-diagonal in the Hilbert space spanned by $|0\rangle$ and $|1\rangle$ and develops along the $\sigma_\pm$ matrices according to:

$$\mathbf{D} = d(\boldsymbol{\epsilon}_a \sigma_- + \boldsymbol{\epsilon}_a^* \sigma_+) \; , \tag{3.149}$$

where we have introduced the notation:

$$q \langle g| \mathbf{R} |e\rangle = d\boldsymbol{\epsilon}_a \; , \tag{3.150}$$

with d being the dipole matrix element of the atomic transition (assumed to be real without loss of generality) and $\boldsymbol{\epsilon}_a$ the unit vector describing the atomic transition polarization. Calling $\mathbf{u}_x$, $\mathbf{u}_y$ and $\mathbf{u}_z$ the unit vectors along the axes Ox, Oy and Oz in real space, we have $\boldsymbol{\epsilon}_a = (\mathbf{u}_x \pm i\mathbf{u}_y)/\sqrt{2}$ for a $\sigma^\pm$-circularly polarized transition. A π-polarized transition corresponds to $\boldsymbol{\epsilon}_a = \mathbf{u}_z$.

The atom–field interaction can be described by a time-independent Hamiltonian, after a simple representation change and a secular approximation. We write $H_a = \hbar\omega_r\sigma_Z/2 + \hbar\Delta_r\sigma_Z/2$, introducing the atom–field detuning:

$$\Delta_r = \omega_{eg} - \omega_r \; . \tag{3.151}$$

We then use an interaction representation with respect to the first part of the atomic Hamiltonian, $\hbar\omega_r\sigma_Z/2$. In the atom–field interaction Hamiltonian, $\sigma_\pm$ are accordingly replaced by $\sigma_\pm \exp(\pm i\omega_r t)$. Among the four terms in the expansion of the $\mathbf{D}\cdot\mathbf{E}_r$ scalar product, two are now time-independent. The two others oscillate at angular frequencies $\pm 2\omega_r$. We can perform the same approximation as the one used in Section 3.1.3 for the coupling of a classical current to a quantum cavity field and neglect the fast oscillating terms. The total Hamiltonian is then:

$$\widetilde{H} = \frac{\hbar\Delta_r}{2}\sigma_Z - i\hbar\frac{\Omega_r}{2}\left[e^{-i\varphi}\sigma_+ - e^{i\varphi}\sigma_-\right] \; , \tag{3.152}$$

where:

$$\Omega_r = \frac{2d}{\hbar}\mathcal{E}_r \boldsymbol{\epsilon}_a^* \cdot \boldsymbol{\epsilon}_r e^{i\varphi_0} \; , \tag{3.153}$$

is the classical Rabi frequency.[23] The phase φ_0 is adjusted to make Ω_r real positive. The phase φ depends on the phase offset between the classical field and the atomic transition dipole. It can be tuned by sweeping the phase of the classical field.

[23] We have considered here the case of an electric dipole transition. A similar two-level Hamiltonian is obtained for a quadrupole transition between $|e\rangle$ and $|g\rangle$ (see Chapter 8), with a different definition for the Rabi frequency Ω_r.

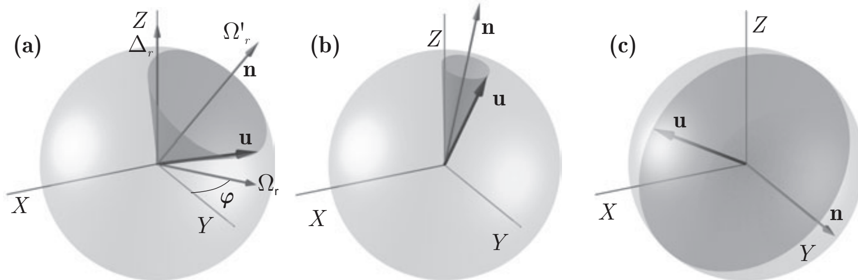

Fig. 3.15 Evolution on the Bloch sphere, viewed in the rotating frame, of the atomic pseudo-spin in an oscillating electric field. The Bloch vector $\mathbf{u}$ precesses at angular frequency Ω'_r around the effective field along $\mathbf{n}$. (a) $\Delta_r \approx \Omega_r$ and arbitray φ. (b) Far off-resonant case. (c) Atom–field resonance ($\Delta_r = 0$) and $\varphi = 0$.

Note that similar equations describe the evolution of a spin subjected to a static magnetic field along OZ and to a time-dependent magnetic field, oscillating along a direction in the equatorial plane of the Bloch sphere. This field can be expanded as the sum of two components rotating in opposite directions in the equatorial plane. The interaction representation used above describes the physics in a frame rotating with the field component quasi-synchronous with the Larmor precession of the spin in the static field. The other component is seen in this frame as a fast rotating field, whose effect can be neglected (hence the name of Rotating Wave Approximation – RWA – given to the secular approximation in this context).

Adopting the nuclear magnetic resonance language, we can write $\widetilde{H}$ in terms of the Pauli matrices:

$$\widetilde{H} = \hbar\frac{\Omega'_r}{2}\boldsymbol{\sigma}\cdot\mathbf{n} \; , \tag{3.154}$$

with $\boldsymbol{\sigma}$ being the formal vector of components σ_X, σ_Y and σ_Z:

$$\Omega'_r = \sqrt{\Delta_r^2 + \Omega_r^2} \; , \tag{3.155}$$

and:

$$\mathbf{n} = \frac{\Delta_r \mathbf{u}_Z - \Omega_r \sin\varphi \, \mathbf{u}_X + \Omega_r \cos\varphi \, \mathbf{u}_Y}{\Omega'_r} \; . \tag{3.156}$$

Here $\mathbf{u}_X$, $\mathbf{u}_Y$ and $\mathbf{u}_Z$ are the unit vectors in the Bloch sphere space, with axes OX, OY and OZ, not to be confused with the real space unit vectors $\mathbf{u}_x$, $\mathbf{u}_y$ and $\mathbf{u}_z$. The Hamiltonian of eqn. (3.154) describes the Larmor precession at the angular frequency Ω'_r of the spin around an effective magnetic field along $\mathbf{n}$. This precession, observed in the frame rotating at angular frequency ω_r around OZ is known in atomic and NMR physics as the 'Rabi oscillation'. We have represented it in figure 3.15 in three different cases: $\Delta_r \approx \Omega_r$ (Fig. 3.15a), $\Delta_r \gg \Omega_r$ (Fig. 3.15b) and $\Delta_r = 0$ (Fig. 3.15c). The vertical component of $\mathbf{n}$ is proportional to Δ_r. Its horizontal component, proportional to the electric field amplitude, makes an angle $\varphi + \pi/2$ with OX.

For a very large atom–field detuning, the effective magnetic field points in a direction close to one of the poles of the Bloch sphere. A spin initially prepared in $|0\rangle$, i.e. at the north pole, undergoes in the frame rotating at ω_r around OZ, a precession of very small amplitude, always remaining close to its initial position (Fig. 3.15b). The spin projection along OZ is nearly constant and there is thus no energy transfer between the field and the atom. A far off-resonant field does not affect appreciably the atomic state. As one tunes the classical field closer to resonance, the direction $\mathbf{n}$ of the effective magnetic field swings away from the polar direction. The circular trajectory of the tip of the Bloch vector widens, bringing it periodically farther and farther from its initial position. For a zero atom–field detuning (resonant case), the Bloch vector rotates at frequency Ω_r around an axis in the equatorial plane (Fig. 3.15c). We choose here for definiteness φ=0. The vector $\mathbf{n}$ is then the unit vector of the OY axis, $\mathbf{u}_Y$. A Bloch vector initially along OZ subsequently precesses along the Bloch sphere's great circle in the XOZ plane. It goes periodically from $|0\rangle$ to $|1\rangle$ and back.

If the Bloch vector is initially parallel or anti-parallel to $\mathbf{u}_Y$, it does not evolve at all. There are thus, in the frame rotating at ω_r around OZ, two stationary states of the atom field coupling, $|0/1_Y\rangle$, eigenstates of the atom–classical field Hamiltonian (see eqn. 3.154) with eigenenergies $\pm\hbar\Omega_r/2$. An arbitrary atomic state can be expressed as a superposition of the $\{|0/1_Y\rangle\}$ eigenstates, with probability amplitudes evolving at frequencies $\pm\Omega_r/2$. The classical Rabi oscillation at Ω_r can thus be interpreted as a quantum interference between these probability amplitudes.

Being merely a spin rotation, the resonant Rabi oscillation provides a simple way to prepare a state with arbitrary polar angles on the Bloch sphere. The interaction during a time $t = \theta/\Omega_r$ with a resonant field having a phase φ performs the rotation:

$$\exp(-i\theta\boldsymbol{\sigma}.\mathbf{n}/2) = \cos(\theta/2)\mathbb{1} - i\sin(\theta/2)\boldsymbol{\sigma}.\mathbf{n} = \begin{pmatrix} \cos(\theta/2) & -\sin(\theta/2)e^{-i\varphi} \\ \sin(\theta/2)e^{i\varphi} & \cos(\theta/2) \end{pmatrix} , \tag{3.157}$$

the first identity resulting from a power series expansion of the exponential, with $(\boldsymbol{\sigma}.\mathbf{n})^2 = \mathbb{1}$. This rotation transforms $|e\rangle = |0\rangle$ into $\cos(\theta/2)\,|0\rangle + \sin(\theta/2)e^{i\varphi}\,|1\rangle$, which is the state whose Bloch vector points in the direction of polar angles θ, φ (see eqn. 2.6, on page 28). In quantum information terms, any single-qubit gate mapping $|0\rangle$ into an arbitrary state can thus be performed by a resonant Rabi oscillation with conveniently chosen θ and φ parameters.

In particular, a $\pi/2$-pulse ($\Omega_r t = \pi/2$) produces the atomic state evolution:

$$|e\rangle \longrightarrow \left|0_{\pi/2,\varphi}\right\rangle = \left[|e\rangle + e^{i\varphi}\,|g\rangle\right]/\sqrt{2}\ ; \qquad |g\rangle \longrightarrow \left[-e^{-i\varphi}\,|e\rangle + |g\rangle\right]/\sqrt{2}\ . \tag{3.158}$$

This transformation mixes $|e\rangle$ and $|g\rangle$ with equal weights. It can be used to prepare an atomic state superposition or to analyse it. In the latter case, the Rabi oscillation is used to map the states $\left|0/1_{\pi/2,\varphi}\right\rangle$ back onto $|e\rangle$ and $|g\rangle$, which can be directly detected. The $\pi/2$-pulse plays a very important role in the Ramsey atomic interferometer (see next paragraph). It behaves as a balanced beam-splitter for the atomic state. It transforms one input state into a coherent quantum superposition, as the optical beam-splitter in Section 3.2.2 transformed an incoming wave packet into a coherent superposition of two wave packets propagating along different paths.[24]

[24] Compare the rotation described by eqn. (3.157) with the unitary beam-splitter operation given by eqn. (3.100) and notice that they are identical provided one makes the notation change $\varphi \rightarrow -\varphi + \pi/2$.

A π-pulse ($\Omega_r t = \pi$) exchanges $|g\rangle$ and $|e\rangle$ according to the transformations:

$$|e\rangle \longrightarrow e^{i\varphi} |g\rangle \ ; \qquad |g\rangle \longrightarrow -e^{-i\varphi} |e\rangle \ , \tag{3.159}$$

which also play an important role in quantum information operations. The $|g\rangle \leftrightarrow |e\rangle$ state exchange can also be performed by an 'adiabatic rapid passage sequence', a procedure again borrowed from nuclear magnetic resonance. The atom, initially in $|g\rangle$ or $|e\rangle$, is subjected to an oscillating field with a strong amplitude and a detuning Δ_r initially set to a very large value. The atomic spin precesses around an effective magnetic field oriented at a very small angle from the Z axis. The detuning Δ_r is then slowly varied, going across resonance and finally reaching a very large value again. The effective magnetic field thus undergoes a slow rotation by an angle π around an axis in the horizontal plane. During this evolution, the Bloch vector continuously precesses around this field. Provided the precession frequency is, at any time, much faster than the field rotation, the spin adiabatically follows the magnetic field and remains nearly aligned with it. It thus ends up pointing along Z, in a direction opposite to the initial one. To an excellent approximation, $|e\rangle$ and $|g\rangle$ are exchanged. The whole sequence duration must be short compared to the atomic relaxation time. This explains the apparent oxymoron ('adiabatic rapid') in the name coined for this process. The adiabatic passage is largely insensitive to the precise field frequency and amplitude. It is much more robust to experimental imperfections than a standard Rabi π-pulse.

Let us finally consider the 2π-pulse ($\Omega_r t = 2\pi$), leading to:

$$|e\rangle \longrightarrow -|e\rangle \ ; \qquad |g\rangle \longrightarrow -|g\rangle \ . \tag{3.160}$$

As expected, the atomic energy is not affected by this 2π-rotation around the effective magnetic field. However, the atomic state experiences a global phase shift by π. This phase shift is a well-known property of a 2π-spin rotation. It will prove very useful in the following.

3.3.3 The Ramsey interferometer

The Ramsey (1985) interferometer is realized by combining two $\pi/2$-Rabi pulses and is closely related to the Mach–Zehnder device, discussed in Section 3.2.3. The first pulse R_1 creates a coherent superposition of atomic states. Before the second pulse R_2 probes it, a tuneable phase shift is applied to the atomic coherence. The operation of the device is sketched in Fig. 3.16(a), using a representation mixing time along the horizontal axis with atomic internal state along the vertical axis. A comparison with Fig. 3.16(b) showing a Mach–Zehnder device makes conspicuous the analogy between the two interferometers.

Let us follow the atomic state transformations for an atom initially in $|e\rangle$. The pulse R_1, with phase $\varphi = 0$, produces the quantum superposition $(|e\rangle + |g\rangle)/\sqrt{2}$. The dephasing element changes it into $(|e\rangle + e^{i\phi}|g\rangle)/\sqrt{2}$. This operation can be achieved by transiently modifying the atomic transition frequency, applying a transient electric or magnetic field. Within an irrelevant global phase factor, this operation produces a phase shift of the atomic coherence, which can be tuned by changing the transient field amplitude or duration. The second pulse R_2, again with phase $\varphi = 0$, then produces the state: